Bone 105 (2017) 42–49

Contents lists available at ScienceDirect

Bone

journal homepage: www.elsevier.com/locate/bone

Activated FGFR3 promotes bone formation via accelerating endochondral ossification in mouse model of distraction osteogenesis

Yusuke Osawa [a,b,*], Masaki Matsushita [a,b], Sachi Hasegawa [c], Ryusaku Esaki [a,b], Masahito Fujio [d], Bisei Ohkawara [b], Naoki Ishiguro [a], Kinji Ohno [b], Hiroshi Kitoh [a]

[a] Department of Orthopaedic Surgery, Nagoya University Graduate School of Medicine, Japan
[b] Division of Neurogenetics, Center for Neurological Diseases and Cancer, Nagoya University Graduate School of Medicine, Japan
[c] Department of Orthopaedic Surgery, Aichi Prefectural Colony Central Hospital, Japan
[d] Department of Oral and Maxillofacial Surgery, Nagoya University Graduate School of Medicine, Japan

ARTICLE INFO

Article history:
Received 18 January 2017
Revised 15 May 2017
Accepted 19 May 2017
Available online 10 August 2017

Keywords:
Achondroplasia
Fibroblast growth factor receptors 3
Mice
Distraction osteogenesis
Bone regeneration

ABSTRACT

Achondroplasia (ACH) is one of the most common short-limbed skeletal dysplasias caused by gain-of-function mutations in the fibroblast growth factor receptors 3 (*FGFR3*) gene. Distraction osteogenesis (DO) is a treatment option for short stature in ACH in some countries. Although the patients with ACH usually show faster healing in DO, details of the newly formed bone have not been examined. We have developed a mouse model of DO and analyzed new bone regenerates of the transgenic mice with ACH (*Fgfr3*^{ach} mice) histologically and morphologically. We established two kinds of DO protocols, the short-DO consisted of 5 days of latency period followed by 5 days of distraction with a rate of 0.4 mm per 24 h, and the long-DO consisted of the same latency period followed by 7 days of distraction with a rate of 0.3 mm per 12 h. The callus formation was evaluated radiologically by bone fill score and quantified by micro-CT scan in both protocols. The histomorphometric analysis was performed in the short-DO protocol by various stainings, including Villanueva Goldner, Safranin-O/Fast green, tartrate-resistant acid phosphatase, and type X collagen. Bone fill scores were significantly higher in *Fgfr3*^{ach} mice than in wild-type mice in both protocols. The individual bone parameters, including bone volume and bone volume/tissue volume, were also significantly higher in *Fgfr3*^{ach} mice than in wild-type mice in both protocols. The numbers of osteoblasts, as well as osteoclasts, around the trabecular bone were increased in *Fgfr3*^{ach} mice. Cartilaginous tissues of the distraction region rapidly disappeared in *Fgfr3*^{ach} mice compared to wild-type mice during the consolidation phase. Similarly, type X collagen-positive cells were markedly decreased in *Fgfr3*^{ach} mice during the same period. *Fgfr3*^{ach} mice exhibited accelerated bone regeneration after DO. Accelerated endochondral ossification could contribute to faster healing in *Fgfr3*^{ach} mice.

1. Introduction

Achondroplasia (ACH) is one of the most common short limbed skeletal dysplasias with an average adult height of 120–130 cm. ACH is caused by gain-of-function mutations in the fibroblast growth factor receptors 3 (*FGFR3*) gene [1,2], which is a negative regulator of endochondral bone development [3]. In addition to rhizomelic shortening of the extremities, relative macrocephaly with frontal bossing, midface hypoplasia, and stenoses of the foramen magnum and spinal canal were associated with patients with ACH [2]. Osteoporotic features were also observed in patients with ACH [4,5] as well as in mouse model of ACH [6]. During the skeletal development, FGFR3 was strongly expressed in resting and proliferating chondrocytes of the growth plates [7]. Additionally, the formation of secondary ossification center was delayed in mouse model of ACH [8,9]. These results indicated that FGFR3 has an essential role for replacement of cartilage with bone during the skeletal development.

Distraction osteogenesis (DO) is a surgical procedure in which new bone formation is induced by gradual distraction of the osteotomy site. DO has widely been accepted in the management of many orthopaedic conditions [10–12]. One of the therapeutic options for short stature in ACH is the lower limb lengthening with DO [13]. The precise mechanism of the new bone formation during DO remains controversial. Endochondral ossification from the central fibrous tissue has been shown in the distraction gap in animal models of DO [14,15]. On the other hand, intramembranous ossification was predominant when a low distraction rate under stable external fixation was applied [16–18].

ACH patients can tolerate extensive lengthening because of their laxity in ligament and soft tissue, and the relatively longer muscles compared with longitudinal bones [19]. Previous report also showed faster

* Corresponding author at: Department of Orthopaedic Surgery, Nagoya University Graduate School of Medicine, 65 Tsurumai-cho, Showa-ku, Nagoya 466-8550, Japan.
E-mail address: yosawa@med.nagoya-u.ac.jp (Y. Osawa).

http://dx.doi.org/10.1016/j.bone.2017.05.016
8756-3282/

bone healing compared to patients with other etiologies in DO [13]. The molecular mechanism of faster bone healing in ACH, however, has not been elucidated.

In the current study, we have established a mouse model of DO, and examined the new bone regenerates of the transgenic mice carrying a heterozygous gain-of-function mutation in FGFR3 (*Fgfr3*^{ach}) morphologically and histologically. We found that activated FGFR3 signaling led to enhance new bone regenerate in the consolidation phase by accelerating endochondral ossification.

2. Materials and methods

2.1. Mice

Fgfr3^{ach} mice (FVB background) were kindly provided by Dr. David M. Ornitz at Washington University [20]. *Fgfr3*^{ach} mice carry *Col2a1* promoter-driven *Fgfr3* carrying p.G380R, which constitutively activates FGFR3 in the growth plate. All experiments were carried out in accordance with protocols approved by the Animal Care and Use Committee of our institution.

2.2. Surgery and distraction protocol

The 4-week-old female *Fgfr3*^{ach} mice and wild-type mice were used for the experiments (Supplemental Fig. S1). The mouse model of DO of the lower limb was produced according to the previously reported protocols [21]. In brief, an anterior longitudinal incision was made on the left lower leg under intraperitoneal anesthesia by using 2.0% Isoflurane. After fibulotomy, 27-gauge needles were inserted at both ends of the tibia. Then, the 27-gauge needles were fixed with the external fixator consisted of two incomplete acrylic resin rings and an expansion screw (Ortho Dentaurum). After complete polymerization, osteotomy was performed at the middle of the diaphysis in the tibia. The wound was closed with a 5–0 nylon suture. Since the rhythm and amount of distraction may affect bone regenerates during DO, we employed two kinds of DO protocols (short-DO and long-DO protocols) (Fig. 1). The short-DO protocol was consisted of 5 days of latency period followed by distraction with a rate of 0.4 mm every 24 h for 5 days. The long-DO protocol was consisted of the same latency period and 7 days of distraction with a rate of 0.3 mm every 12 h (0.6 mm / 24 h). As a result, longer and faster distraction was acquired in the long-DO than in the short-DO. The day 0 was defined as the day at the end of distraction. The external fixators were removed at day 28 of consolidation phase in both models.

We analyzed a total of 17 kinships, including 31 *Fgfr3*^{ach} mice and 35 wild-type mice. We first performed short-DO according to the previous report [21]. The five *Fgfr3*^{ach} mice and seven wild-type mice were subjected to a soft x-ray and micro-CT scan at each time point individually. We next evaluated the histological sections from 20 *Fgfr3*^{ach} mice and 20 wild-type mice at each time point during the short-DO protocol. We further performed radiological analyses of six *Fgfr3*^{ach} mice and eight wild-type mice treated with the long-DO protocol.

2.3. Radiographic analysis

Under general anesthesia, the mice were subjected to a soft x-ray (30 kV, 5 mA for 20 s; SOFTEX Type CMB-2; SOFTEX) after completion of distraction at days 4, 7, 14, 28, and 42. The callus formations were quantified by bone fill scores. Bone fill scores of 0, 1, 2, and 3 represent 0%, 0–50%, 50–100%, and 100% bone fills, respectively [24,25]. Based on lateral radiographic images taken at day 42, the bone union was assessed by the formation of seamless bridging callus. The number of bridging cortical line was counted: score 0 represents nonunion of both anteroposterior cortices, score 1 represents union of either anterior or posterior hemicortex, and score 2 represents union of both anteroposterior cortices [26]. We also measured the distance between the proximal and distal fragment from the lateral x-ray images at day 7 to confirm that the distraction was done successfully in both protocols.

Micro-computed tomography (micro-CT) scan (Al ± Cu filter, voxel size 0.9 μm, 80 kV, 313 μA for 0.203 s; SkyScan1176, Bruker) examinations were performed at days 7 and 14 under general anesthesia. After reconstruction using the Skyscan NRecon software, the images were analyzed by three-dimensional (3D) algorithms in Skyscan CTAn software according to the manufacturer's instructions. Region of interest (ROI) was determined as the distraction region surrounded by the outlined

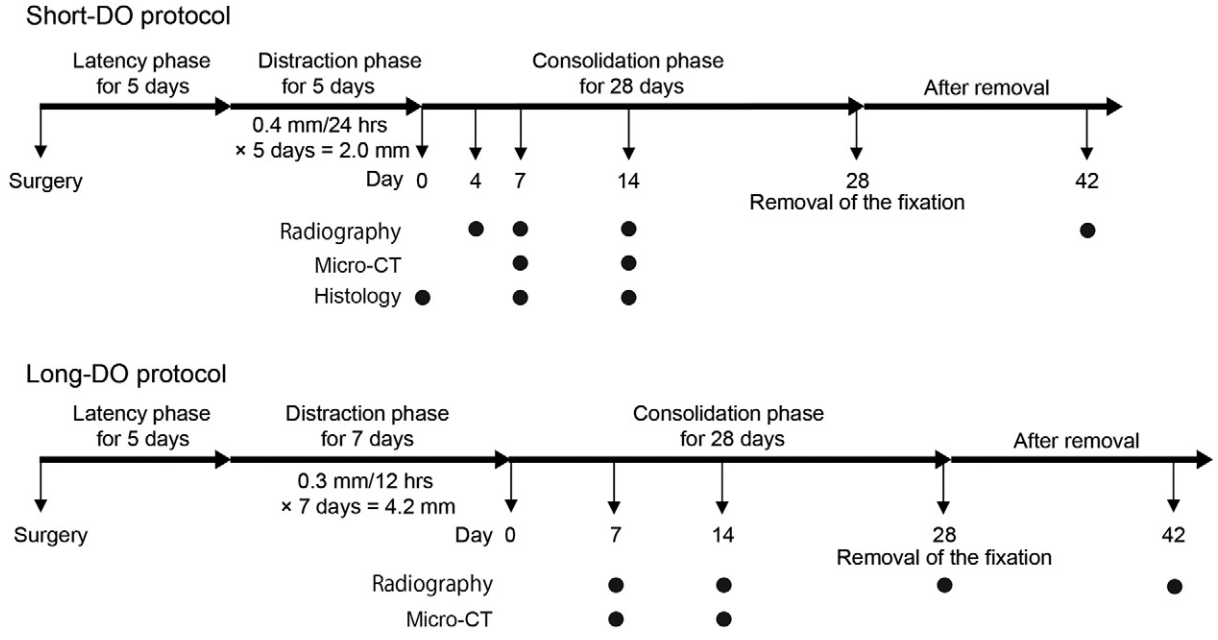

Fig. 1. Protocols of distraction osteogenesis (DO). After the surgery, a 5-day-latency phase was followed by the distraction phase for 5 days with 0.4 mm/24 h of distraction rate (short-DO) or for 7 days with 0.3 mm/12 h of distraction rate (long-DO). The total increased lengths were theoretically 2.0 mm in short-DO protocol and 4.2 mm in long-DO protocol, respectively. The day 0 was defined as the day of completion of distraction. The external fixators were removed at day 28. The dates of each analysis are indicated by closed circles.

periosteum from the proximal and distal ends according to the previous studies [22,23], and bone volume (BV) and BV to total volume ratio (BV/TV) were measured.

2.4. Histomorphometric analysis

The distracted tibiae were stained with Villanueva Goldner at day 7 of the short-DO protocol in order to investigate new bone formation in decalcified tissues. Specimens were fixed with 70% ethanol for 3 days, dehydrated through graded ethanol series, and embedded in methyl methacrylate without decalcification (Tokai Cytopathology Institute, Japan). Calcified and osteoid area were quantified by Image J software according to the previous studies [27,28], in a blinded manner. The analyzed parameters included bone volume/distraction area, osteoid volume/distraction area, BV/TV, osteoid volume/tissue volume (OV/TV), osteoid volume/bone volume (OV/BV), and osteoid surface/bone surface (OS/BS) according to the previous studies [26,28,29].

Additionally, at days 0, 7, and 14 of the short-DO protocol, distracted tibiae were fixed with 4% paraformaldehyde and decalcified at 4 °C in 10% EDTA solutions for 3 weeks. Specimens were dehydrated in a graded ethanol series and stained in paraffin. After slicing into 6 μm, Safranin-O/Fast green (SO/FG) staining was performed. For immunohistochemistry, the sections were stained with antibodies specific for tartrate-resistant acid phosphatase (TRAP) and type X collagen (Col X) (1:250 dilution, Abcam). The most central sections of the medullary cavity were chosen for the histomorphometric analyses. The three arbitrary parts in the center of new bone formation at day 7 were chosen for counting the number of osteoclasts in TRAP staining. The areas stained with SO/FG and Col X were measured by Image J software.

2.5. Statistics

Data are expressed as mean ± SD. Statistical analyses were carried out using unpaired Student *t*-test, Fisher's exact test, or two-way ANOVA.

3. Results

3.1. Callus formation was accelerated in DO of the *Fgfr3*^{ach} mice

Bone alignment of the distracted tibiae was maintained after distraction in both protocols, suggesting that successful DO was done by our experimental model. Actually, the average distraction gap in the short-DO at day 7 was 1.88 mm in wild-type mice and 1.85 mm in *Fgfr3*^{ach} mice, respectively. In the long-DO, the average distraction gap was 4.12 mm in wild-type mice and 4.06 mm in *Fgfr3*^{ach} mice. There were no statistical differences between both groups (Supplemental Fig. S2). Callus formation was gradually increased in wild-type mice and *Fgfr3*^{ach} mice during the consolidation phase. We quantified callus formation in DO by the bone fill scores. The *Fgfr3*^{ach} mice in the short-DO protocol showed significantly higher bone fill scores than wild-type mice at days 4, 7, and 14 (Fig. 2A). Similarly, the bone fill score in the long-DO protocol was significantly higher in *Fgfr3*^{ach} mice than in wild-type mice at days 7 and 14 (Fig. 2B).

Next, we evaluated maturation of the new bone regenerates after removal of the external fixators at day 42. The distracted bones were united with almost good alinement in *Fgfr3*^{ach} mouse while angular deformities were observed in wild-type mouse in both protocols (Supplemental Figs. S3A and C). We measured the number of uniting callus, and observed that *Fgfr3*^{ach} mice tended to have more united calluses compared to wild-type mice although there was no statistical difference between both mice (Supplemental Figs. S3B and D).

3.2. Enhanced bone formation in *Fgfr3*^{ach} mice was confirmed by the quantitative 3D-CT analysis

We next quantified the callus formation using the micro-CT scan. Representative images of the distraction area demonstrated elevated bone formation at days 7 and 14 in both protocols (Figs. 3A and C). The BV and BV/TV were significantly increased in *Fgfr3*^{ach} mice in the short-DO protocol (Fig. 3B). In the long-DO protocol, BV and BV/TV were significantly larger in *Fgfr3*^{ach} mice than in wild-type mice (Fig. 3D). There were no significant differences in BV/TV between the short- and long-DO protocols in wild-type mice as well as in *Fgfr3*^{ach} mice.

3.3. Both osteoblasts and osteoclasts were increased in *Fgfr3*^{ach} mice at day 7 after completion of distraction

We next performed histomorphometric analyses of the distraction area at day 7 based on the Villanueva Goldner staining. Callus formation was more prominent in *Fgfr3*^{ach} mice compared to wild-type mice (Fig. 4A). The BV and OV per distraction area were significantly increased in *Fgfr3*^{ach} mice than in wild-type mice (Fig. 4B). High magnification images of the center of newly formed bone demonstrated a large number of osteoblasts surrounding the osteoid in *Fgfr3*^{ach} mice (Fig. 4C). Furthermore, osteoid-related parameters, including OV/TV, OV/BV, and OS/BS, were significantly increased in *Fgfr3*^{ach} mice (Fig. 4D). The osteoclast numbers in TRAP staining were significantly increased in *Fgfr3*^{ach} mice than in wild-type mice (Figs. 4E and F).

3.4. Endochondral ossification of the distraction area was promoted in *Fgfr3*^{ach} mice

We next evaluated the endochondral ossification process in DO by SO/FG staining. Within the distracted gap in both wild-type and mutant mice, cartilaginous tissues with angiogenesis at the boundary region were prominent at the beginning of consolidation phase, indicating that DO produced endochondral ossification. (Supplemental Fig. S4) On the other hand, the cartilage areas gradually disappeared as the union progressed (Fig. 5A). Quantification of the SO/FG staining demonstrated significantly decreased cartilage areas in *Fgfr3*^{ach} mice than in wild-type mice at day 7 (Fig. 5B). The expression of Col X of both treatment groups was upregulated at day 0 and decreased at day 7 (Fig. 5C). Quantification of the Col X expression showed that faster disappearance of the Col X-positive cells was observed in *Fgfr3*^{ach} mice (Fig. 5D).

4. Discussion

The mouse model of DO has rarely been reported in the literature [21–24]. We confirmed successful DO technique using an acrylic resin external fixator with the 27 gauge needles. Experimental mouse models are beneficial because we can elucidate disease-specific pathophysiology using transgenic mice. In the current study, we quantitatively exhibited significantly faster healing in DO using *Fgfr3*^{ach} mice, which expresses the human achondroplasia mutation G380R.

Factors for contributing to intramembranous and endochondoral ossification in DO have been reported, including the stability of the distraction devices, timing and rate of distraction, and species-related difference [30–32]. Forriol et al. demonstrated that moderate amount of cartilage tissue was observed in all of the sheep DO models irrespective of distraction rate [33]. Fujio et al. demonstrated that endochondral ossification was more prominent in faster rate of distraction than in lower rate of distraction [21]. Yasui et al. using a rat model of DO, reported that endochondral ossification was mainly observed in the distraction periods while membranous ossification was predominant during the consolidation periods associated with significant decrease in cartilage area [34]. Although we have not examined the histology of the distracted callus during the distraction phase, abundant cartilage tissue

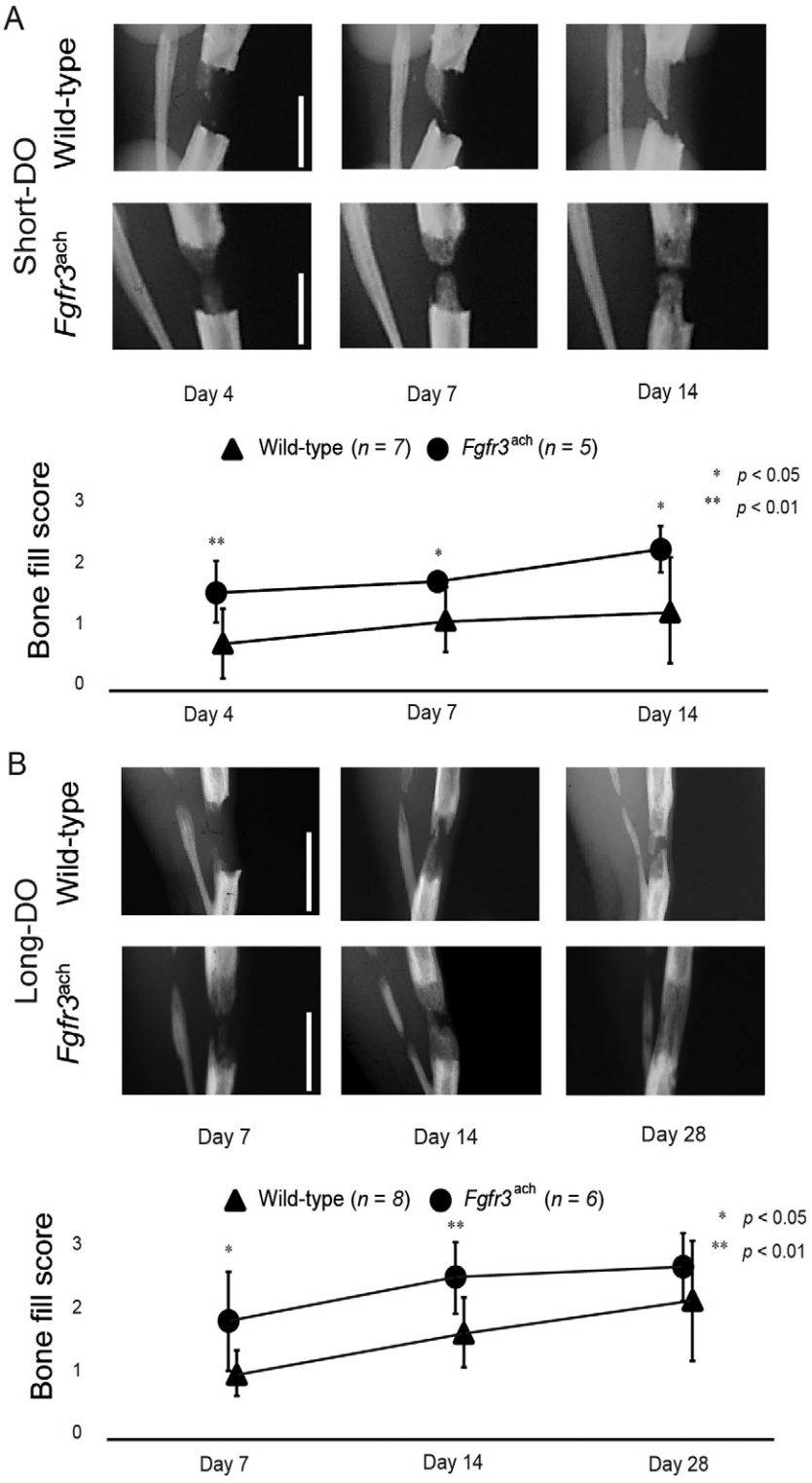

Fig. 2. Radiographic calluses were increased in *Fgfr3*^{ach} mice after the distraction. (A) Representative radiographs with the short-DO protocol. Bone fill score was employed to quantify the bony callus during DO. Bone fill scores were significantly increased in *Fgfr3*^{ach} mice ($n = 5$) than those in wild-type mice ($n = 7$) at days 4, 7, and 14. Scale bares indicate 2 mm. (B) Representative radiographs with the long-DO protocol. Bone fill scores were also increased in *Fgfr3*^{ach} mice ($n = 6$) than those in wild-type mice ($n = 8$) at days 7, 14, and 28, while there was no statistical difference at day 28. Scale bares indicate 4 mm. Mean and SD are indicated. The statistical differences were analyzed by unpaired *t*-test. n.s., not significant.

observed at the end of distraction indicated that endochondral ossification was also predominant during distraction phase in the current DO model, which may be due to the instability of the distraction devices.

Deng et al. demonstrated that disrupting murine *Fgfr3* gene revealed an enhanced and prolonged endochondral bone growth with expansion of proliferating and hypertrophic chondrocytes in growth plate [3]. In contrast, *Fgfr3*^{ach} mice showed short-statured phenotype with inhibited chondrocyte proliferation and differentiation [20]. These results indicated that FGFR3 is a negative regulator of endochondral ossification in skeletal development. In contrast, Nakajima et al. showed that FGFR3 was predominantly expressed in prehypertrophic chondrocytes during fracture repair, indicating differential patterns of FGFR3 expression

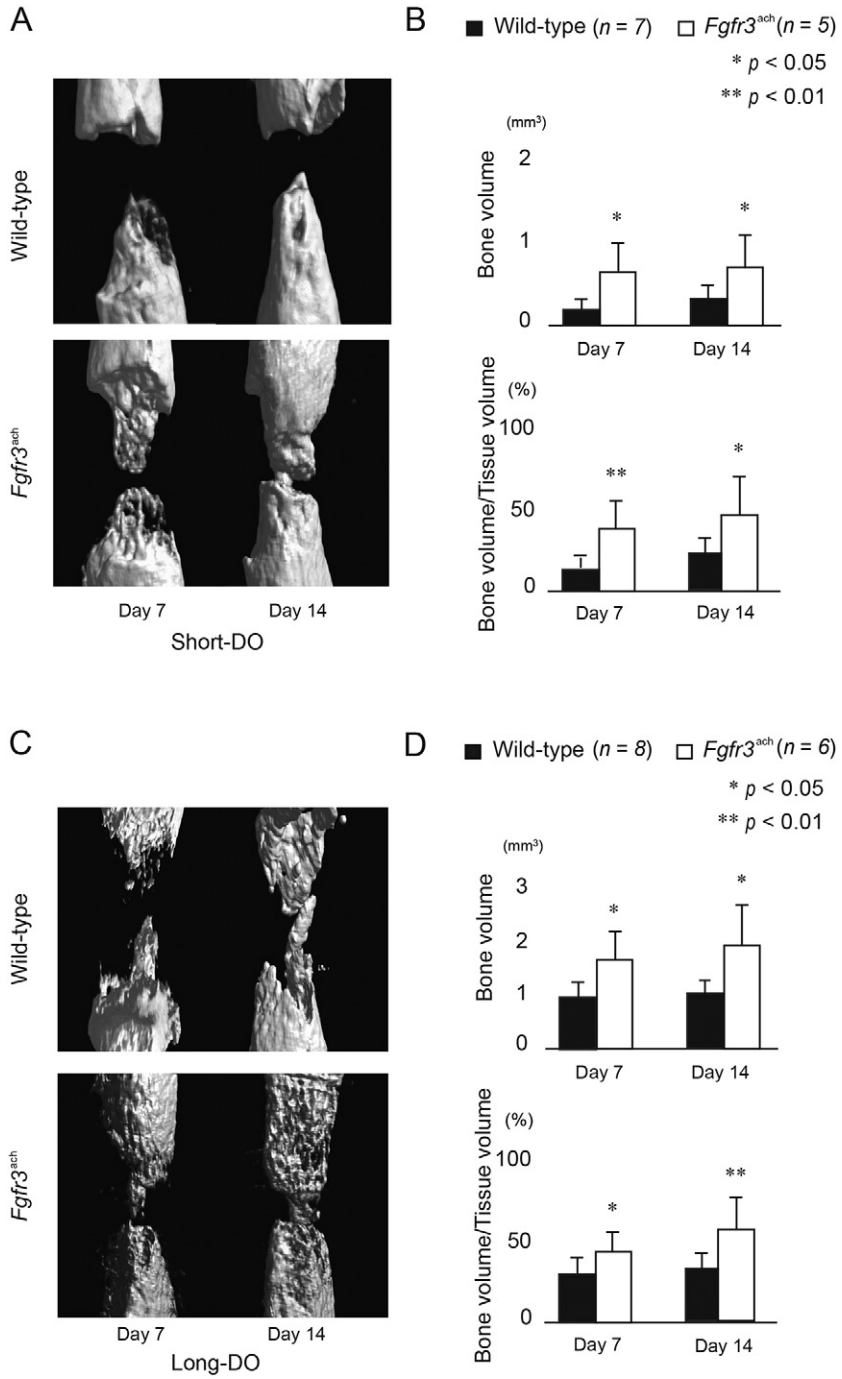

Fig. 3. Accelerated bone formation in *Fgfr3*^{ach} mice was confirmed by micro-CT scan. (A, C) Representative 3D images reconstructed from micro-CT scan showing upregulated bone formation in *Fgfr3*^{ach} mice in the distraction space at days 7 and 14 in the short-DO model (A) and the long-DO model (C). (B, D) Mean and SD of individual bone parameters of the reconstructed 3D images in the short-DO model (B) and the long-DO model (D) are plotted. In the short-DO model, individual parameters were significantly elevated in *Fgfr3*^{ach} mice ($n = 5$) than in wild-type mice ($n = 7$) at days 7 and 14. Similarly in the long-DO model, these parameters were significantly increased in *Fgfr3*^{ach} mice ($n = 6$) than in wild-type mice ($n = 8$). Statistical differences were analyzed by unpaired *t*-test.

between skeletal development and fracture repair [7]. They also demonstrated that TUNEL-positive apoptotic cells were localized to hypertrophic chondrocyte, and suggested that role of FGFR3 during fracture repair is to induce apoptosis of hypertrophic chondrocytes, thereby promoting endochondral ossification. Similar to the fracture repair, disappearance of the cartilage tissue and replacement to the bony tissue were rapidly observed in ACH mice compared to the wild-type mice during the consolidation phase. These results indicate that accelerated endochondral ossification process within the distracted callus contributes to promotion of new bone formation during DO in ACH.

Chondrocyte-specific activation of Fgfr3 in mice enhanced endochondral ossification at the synchondroses around the spine and cranial base, resulting in the stenoses of spinal canal and foramen magnum [35]. In the current study, not only calcified bone but also osteoid tissue was significantly increased in *Fgfr3*^{ach} mice, suggesting that increased FGFR3 in chondrocytes upregulated osteoblast differentiation during the new bone formation. On the other hand, Su et al. demonstrated the direct positive regulation of FGFR3 on osteoclastic bone resorption [36]. We observed the increased numbers of osteoclasts, as well as osteoblasts, at the distraction callus where active bone formation

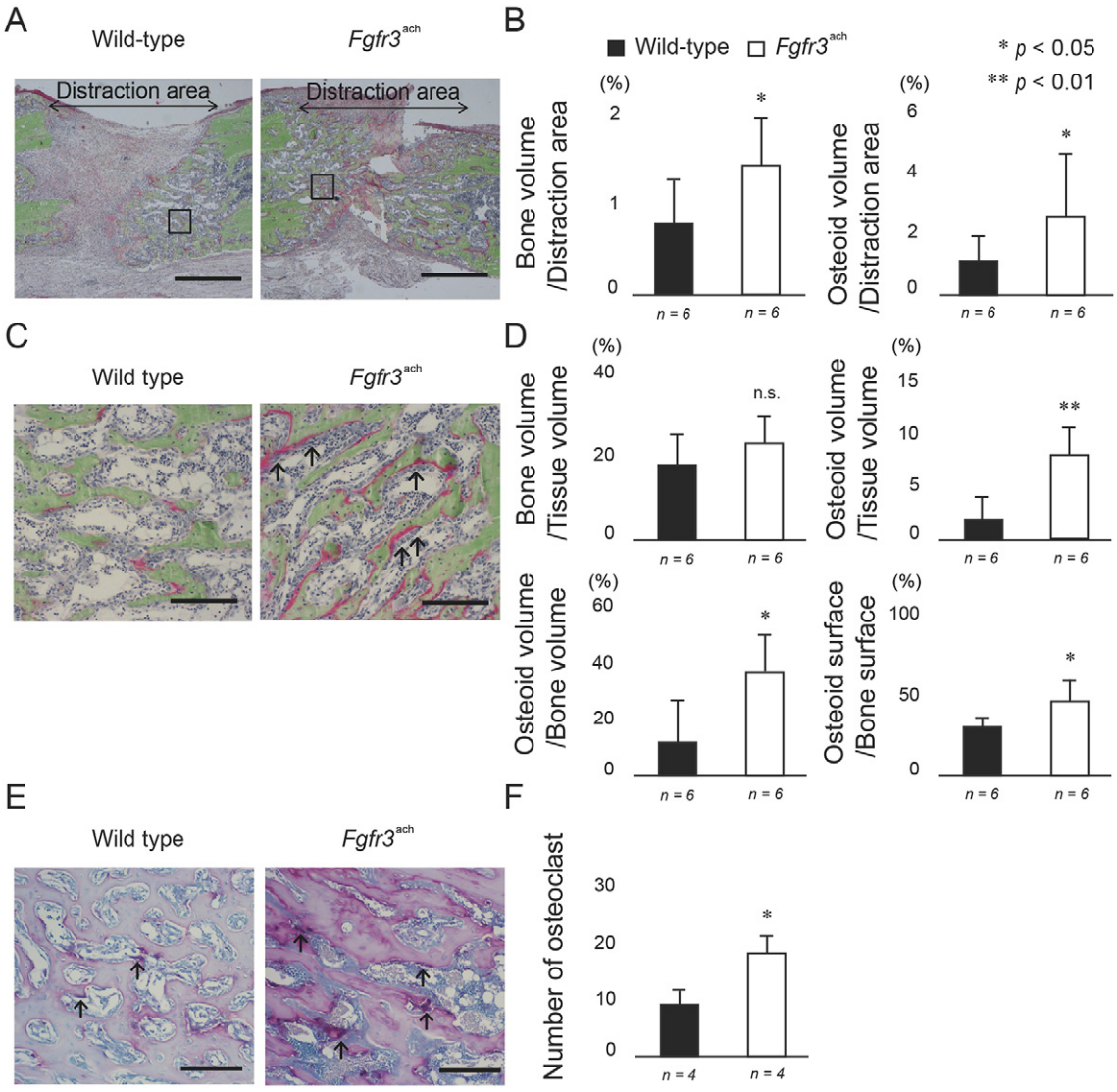

Fig. 4. Enhanced bone and osteoid volume were associated with increased number of osteoblasts and osteoclasts in *Fgfr3*^{ach} mice ($n = 6$) compare to wild-type mice ($n = 6$) at day 7. (A) Representative undecalcified histology of distracted area stained with Villanueva Goldner staining. Green signals show calcified bones. Red signals show osteoid bones. Purple signals show osteoclasts. Squared parts are magnified in (C). Scale bares indicate 1 mm. (B) Mean and SD of bone volume/distraction area and osteoid volume/distraction area are plotted. (C) Magnification images showing increased osteoid area in *Fgfr3*^{ach} mouse in the central part of newly formed bone. There were a lot of osteoblasts (*arrow*) around osteoid bone in *Fgfr3*^{ach} mice compare to wild-type mice. Scale bares indicate 40 μm. (D) Mean and SD of indicated parameters within the ROI are plotted. Osteoid-related parameters other than bone volume/tissue volume were significantly increased in *Fgfr3*^{ach} mice than in wild-type mice. (E) Representative high magnificent images of TRAP staining in the central part of newly formed bone indicating a lot of osteoclasts (*arrow*) around osteoid bone in *Fgfr3*^{ach} mice ($n = 4$) compare to wild-type mice ($n = 4$). (F) Mean and SD of the number of osteoclasts within the ROI are plotted. The number of osteoclasts was significantly increased in *Fgfr3*^{ach} mice than in wild-type mice. Statistical differences were analyzed by unpaired *t*-test.

took place in *Fgfr3*^{ach} mice. During endochondral ossification in bone development, osteoclasts degrade the calcified cartilage extracellular matrix, followed by recruitment of osteoprogenitors to form bone tissue replacing the calcified cartilage template [37,38]. These findings indicate that upregulation of both osteoblasts and osteoclasts at the trabecular bone region can contribute to faster maturation of callus in ACH.

Thompson et al. demonstrated that endochondral ossification was mainly observed in an unstabilized fracture, while intramembraneous ossification was predominant in a stabilized fracture [39]. Lack of stability may be related to predominance of endochondral ossification during the distraction phase. Intramembranous ossification, on the other hand, could be stimulated after the end of distraction by increased stability. Su et al. employed non-stabilized fracture model for evaluating bone regeneration in abnormally activated FGFR3 signaling [40]. They demonstrated that cartilage area, which was significantly increased in *Fgfr3*$^{G369C/+}$ mice than in wild-type mice, resided within the callus for a long time after fracture, resulting in impaired fracture repair. On the other hand, bone regenerations were accelerated in *Fgfr3*^{ach} mice through enhanced endochondral ossification process in the current DO model.

There are several limitations in the current study. First, we performed histological analysis on distracted bones only in short-DO protocol. Long-DO protocol or slower distraction rates may reveal different histologies. Second, we removed the fixation at 28 days after completion of distraction. Most distracted bones in wild-type mice revealed pseudarthlosis probably due to the short period of consolidation phase. Third, we performed 2.0 mm and 4.2 mm of lengthening in short-DO and long-DO protocol, respectively, which seems to be smaller than that of DO in ACH. Further studies for investigating the mechanism of DO may develop new therapeutic approach for enhancing bone generation during DO in many orthopaedic conditions.

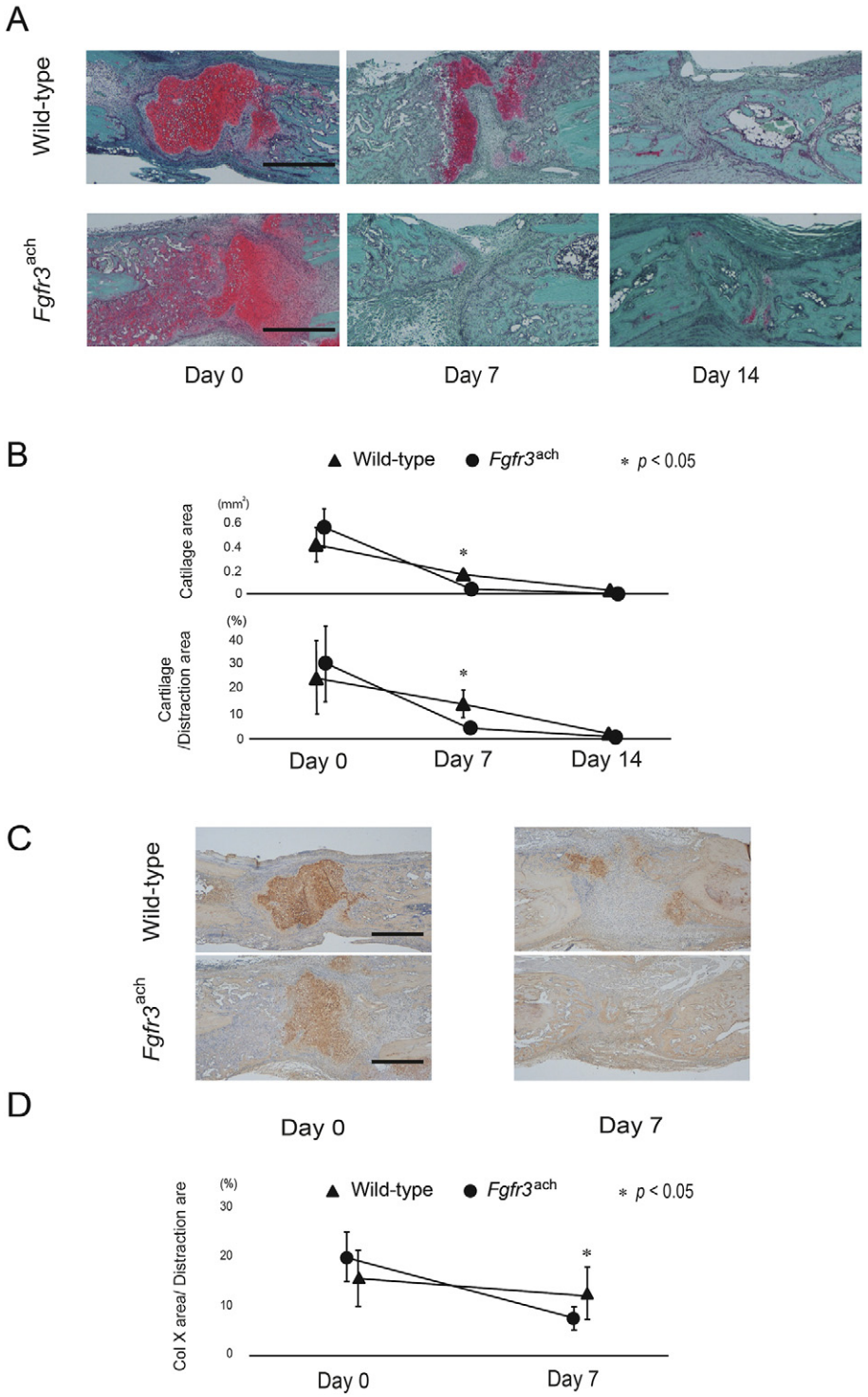

Fig. 5. Endochondral ossification was accelerated in *Fgfr3*^{ach} mice during the consolidation phase. (A) Representative images of Safranin-O/Fast green (SO/FG) staining. Red signals show cartilage. Scale bares indicate 1 mm. (B) Mean and SD of cartilaginous area and cartilaginous area/distraction area of (A) are indicated. (A, B) Cartilaginous tissues predominantly observed at day 0 were decreased in wild-type mouse ($n = 6$) and almost disappeared in *Fgfr3*^{ach} mouse ($n = 6$) at day 7. Cartilaginous area was no longer observed at day 14 in both groups ($n = 4$). (C) Representative immunohistochemical images of Col X staining. Similarly, abundant Col X positive cells at day 0 were decreased in wild-type mice and almost disappeared in *Fgfr3*^{ach} mice at day 7. Scale bares indicate 40 μm. (D) The quantification of Col X-positive area/distraction area indicating significant decrease in Col X positive cells in *Fgfr3*^{ach} mice at day 7 ($n = 4$) Mean and SD are indicated. The statistical differences were analyzed by unpaired *t*-test.

Supplementary data to this article can be found online at http://dx.doi.org/10.1016/j.bone.2017.05.016.

Disclosures

All authors state that they have no conflicts of interest.

Acknowledgments

This research was funded by Grants-in-Aid from the Ministry of Education, Culture, Sports, Science and Technology of Japan Grant Number 15K10439. We thank Dr. David M. Ornitz at Washington University for providing the *Fgfr3*^{ach} mice. YO, MM, and HK designed the research.

YO, MM, SH, and MF performed the experiments and collected data. RE managed animals. YO, MM, BO, NI, KO, and HK analyzed and interpreted the data. The manuscript was drafted by TO and MM, and revised by KO and HK. All authors approved the final version of the article. NI and HK take responsibility for the integrity of the work.

References

[1] D.K. Waller, A. Correa, T.M. Vo, et al., The population based prevalence of achondroplasia and thanatophoric dysplasia in selected regions of the US, Am. J. Med. Genet. A 146 (2008) 2385–2389.
[2] W.A. Horton, J.G. Hall, J.T. Hecht, Achondroplasia. Lancet. 370 (9582) (2007) 162–172.
[3] C. Deng, A. Wynshaw-Boris, F. Zhou, et al., Fibroblast growth factor receptor 3 is a negative regulator of bone growth, Cell 84 (1996) 911–921.
[4] M. Matsushita, H. Kitoh, K. Mishima, et al., Low bone mineral density in achondroplasia and hypochondroplasia, Pediatr. Int. 58 (2016) 705–708.
[5] E.S. Arita, M.G. Pippa, M. Marcucci, et al., Assessment of osteoporotic alterations in achondroplastic patients: a case series, Clin. Rheumatol. 32 (2013) 399–402.
[6] N. Su, Q. Sun, C. Li, et al., Gain-of-function mutation in FGFR3 in mice leads to decreased bone mass by affecting both osteoblastogenesis and osteoclastogenesis, Hum. Mol. Genet. 19 (2010) 1199–1210.
[7] A. Nakajima, S. Shimizu, H. Moriya, et al., Expression of fibroblast growth factor receptor-3 (FGFR3), signal transducer and activator of transcription-1, and cyclin-dependent kinase inhibitor p21 during endochondral ossification: differential role of FGFR3 in skeletal development and fracture repair, Endocrinology 144 (2003) 4659–4668.
[8] A. Yasoda, Y. Komatsu, H. Chusho, et al., Overexpression of CNP in chondrocytes rescues achondroplasia through a MAPK-dependent pathway, Nat. Med. 10 (2004) 80–86.
[9] F. Lorget, N. Kaci, J. Peng, et al., Evaluation of the therapeutic potential of a CNP analog in a Fgfr3 mouse model recapitulating achondroplasia, Am. J. Hum. Genet. 91 (2012) 1108–1114.
[10] D. Paley, Problems, obstacles, and complications of limb lengthening by the Ilizarov technique, Clin. Orthop. Relat. Res. 250 (1990) 81–104.
[11] C.F. Moseley, Leg lengthening. A review of 30 years, Clin. Orthop. Relat. Res. 247 (1989) 38–43.
[12] K. Korzinek, S. Tepic, S.M. Perren, Limb lengthening and three-dimensional deformity corrections: a retrospective clinical study, Arch. Orthop. Trauma Surg. 109 (1990) 334–340.
[13] S.J. Kim, W. Pierce, S. Sabharwal, The etiology of short stature affects the clinical outcome of lower limb lengthening using external fixation. A systematic review of 18 trials involving 547 patients, Acta Orthop. 85 (2014) 181–186.
[14] H. Kojimoto, N. Yasui, T. Goto, et al., Bone lengthening in rabbits by callus distraction. The role of periosteum and endosteum, J. Bone Joint Surg. (Br.) 70 (1988) 543–549.
[15] M. Ohyama, Y. Miyasaka, M. Sakurai, et al., The mechanical behavior and morphological structure of callus in experimental callotasis, Biomed. Mater. Eng. 4 (1994) 273–281.
[16] T.J. Kallio, M.V. Vauhkonen, J.I. Peltonen, et al., Early bone matrix formation during distraction. A biochemical study in sheep, Acta Orthop. Scand. 65 (1994) 467–471.
[17] G.A. Ilizarov, The tension-stress effect on the genesis and growth of tissues: part II. The influence of the rate and frequency of distraction, Clin. Orthop. Relat. Res. 239 (1989) 263–285.
[18] R. Rivas, F. Shapiro, Structural stages in the development of the long bones and epiphyses: a study in the New Zealand white rabbit, J. Bone Joint Surg. Am. 84 (2002) 85–100.
[19] D. Paley, Current techniques of limb lengthening, J. Pediatr. Orthop. 8 (1988) 73–92.
[20] M.C. Naski, J.S. Colvin, J.D. Coffin, et al., Repression of hedgehog signaling and BMP4 expression in growth plate cartilage by fibroblast growth factor receptor3, Development 125 (1998) 4977–4988.
[21] M. Fujio, A. Yamamoto, Y. Ando, et al., Stromal cell-derived factor-1 enhances distraction osteogenesis-mediated skeletal tissue regeneration through the recruitment of endothelial precursors, Bone 49 (2011) 693–700.
[22] D.S. Perrien, K.M. Nicks, L. Liu, et al., Inhibin A enhances bone formation during distraction osteogenesis, J. Orthop. Res. 30 (2012) 288–295.
[23] K.C. Stine, E.C. Wahl, L. Liu, et al., Cisplatin inhibits bone healing during distraction osteogenesis, J. Orthop. Res. 32 (2014) 464–470.
[24] M. Gdalevitch, B. Kasaai, N. Alam, et al., The effect of heparan sulfate application on bone formation during distraction osteogenesis, PLoS One 8 (2013), e56790. .
[25] M.J. Troulis, C. Coppe, M.J. O'Neill, et al., Ultrasound: assessment of the distraction osteogenesis wound in patients undergoing mandibular lengthening, J. Oral Maxillofac. Surg. 61 (2003) 1144–1149.
[26] K. Mishima, H. Kitoh, B. Ohkawara, et al., Lansoprazole upregulates polyubiquitination of the TNF receptor-associated factor 6 and facilitates Runx2-mediated osteoblastogenesis, EBioMedicine. 2 (2015) 2046–2061.
[27] K. Ikuta, H. Urakawa, E. Kozawa, et al., In vivo heat-stimulus-triggered osteogenesis, Int. J. Hyperth. 31 (2015) 58–66.
[28] H. Akagi, H. Ochi, S. Soeta, et al., A comparison of the process of remodeling of hydroxyapatite/poly-D/L-lactide and beta-tricalcium phosphate in a loading site, Biomed. Res. Int. 2015 (2015) 730105.
[29] D.W. Dempster, J.E. Compston, M.K. Drezner, et al., Standardized nomenclature, symbols, and units for bone histomorphometry: a 2012 update of the report of the ASBMR Histomorphometry nomenclature committee, J. Bone Miner. Res. 28 (2013) 2–17.
[30] B. Fink, C. Pollnau, M. Vogel, et al., Histomorphometry of distraction osteogenesis during experimental tibial lengthening, J. Orthop. Trauma 17 (2003) 113–118.
[31] V. Kusec, M. Jelic, F. Borovecki, et al., Distraction osteogenesis by Ilizarov and unilateral external fixators in a canine model, Int. Orthop. 27 (2003) 47–52.
[32] G. Li, A.H. Simpson, J.T. Triffitt, The role of chondrocytes in intramembranous and endochondral ossification during distraction osteogenesis in the rabbit, Calcif. Tissue Int. 64 (1999) 310–317.
[33] F. Forriol, L. Denaro, U.G. Longo, H. Taira, N. Maffulli, V. Denaro, Bone lengthening osteogenesis, a combination of intramembranous and endochondral ossification: an experimental study in sheep, Strategies Trauma Limb Reconstr. 5 (2010) 71–78.
[34] N. Yasui, M. Sato, T. Ochi, et al., Three modes of ossification during distraction osteogenesis in the rat, J. Bone Joint Surg. (Br.) 79 (1997) 824–830.
[35] T. Matsushita, W.R. Wilcox, Y.Y. Chan, et al., FGFR3 promotes synchondrosis closure and fusion of ossification centers through the MAPK pathway, Hum. Mol. Genet. 18 (2009) 227–240.
[36] N. Su, X. Li, Y. Tang, J. Yang, et al., Deletion of FGFR3 in osteoclast lineage cells results in increased bone mass in mice by inhibiting osteoclastic bone resorption, J. Bone Miner. Res. 31 (2016) 1676–1687.
[37] G. Karsenty, E.F. Wagner, Reaching a genetic and molecular understanding of skeletal development, Dev. Cell 2 (2002) 389–406.
[38] X. Du, Y. Xie, C.J. Xian, L. Chen, Role of FGFs/FGFRs in skeletal development and bone regeneration, J. Cell. Physiol. 227 (2012) 3731–3743.
[39] Z. Thompson, T. Miclau, D. Hu, J.A. Helms, A model for intramembranous ossification during fracture healing, J. Orthop. Res. 20 (2002) 1091–1098.
[40] N. Su, J. Yang, Y. Xie, et al., Gain-of-function mutation of FGFR3 results in impaired fracture healing due to inhibition of chondrocyte differentiation, Biochem. Biophys. Res. Commun. 376 (2008) 454–459.
[41] M. Matsushita, S. Hasegawa, H. Kitoh, et al., Meclozine promotes longitudinal skeletal growth in transgenic mice with achondroplasia carrying a gain-of-function mutation in the FGFR3 gene, Endocrinology 156 (2015) 548–554.